Advanced Antenna Modelling Tool for Performance Verification and Diagnosis

Executive Summary Report

ESA Contract No. AO/1-10116/19/NL/AS

***Abstract*—This document summarises the work performed within the ESA Contract No. AO/1-10116/19/NL/AS. It discusses the design and implementation of a new software tool intended for computing and representing the uncertainties of an antenna's performance caused by the stochastic behaviour of design variables of the system. The mathematical algorithms implemented in the tool allow for a very general formulation, where uncertainty can be added to both geometrical and electrical parameters of the system. Further, the algorithms are designed with speed and accuracy in mind, resulting in trustworthy statistical quantities such as confidence intervals. To validate the software, several testcases were designed and the results are compared to both analytical and measured data. The results show impressive performance by the software tool, allowing for better antennas to be produced by taking into account realistic, rather than ideal, performance of a manufactured antenna.**

***Index Terms*—Uncertainty quantification, space applications, antenna design software**

I. Introduction

Designing antenna systems for modern telecommunication or earth observation applications entails stringent performance requirements and strict error budgets. As the systems become increasingly complex and involve many subsystems, the need for accurate and reliable quantification of the imperfections involved in the error budgets becomes greater and greater. In particular, for concepts such as unfurlable reflectarrays or unfurlable reflectors, where in-flight deployment is used, detailed mechanical and thermal studies are required, all of which provide parameter ranges rather than specific parameter values. Further, for high-accuracy applications such as deep-space communication, even minor imperfections can have devastating consequences if not taken into account.

Modern computational electromagnetics software makes it possible for the RF engineer to simulate a large number of the mechanical designs, and in some cases the software can allow fully automatic optimization to attain optimal performance. However, when it comes to quantifying the uncertainty, e.g., the performance degradation introduced by mechanical imperfections, the engineers are currently on their own.

If the engineers apply some form of uncertainty analysis, most will resort to simply running a very large number of simulations with random errors added sporadically to the system, and then perform some statistical examination on that data, a so-called *Monte-Carlo* simulation. The downsides to this approach are clear: A very large number of simulations are required, and the risk of user error is high. Further, the statistical accuracy is extremely poor, which could cause misleading conclusions about the final performance when the antenna is deployed.

The objective of the present activity has been to develop a powerful software package that allows antenna designers to study the impact of uncertainties already in the design phase. The software is closely coupled with TICRAs existing software tools, and is therefore able to analyse antennas commonly used for satellite communication payloads or scientific instruments, including passive microwave components, feeds, reflectors, arrays, reflectarrays, etc. Further, the software is able to assess uncertainties related to structural antenna elements and the satellite platform. The software allows uncertainties to be associated with all geometrical and electrical input parameters and computes statistical output of all performance parameters of interest.

The major steps involved in the software development have been the following:

1) Evaluate the most efficient algorithms for uncertainty qualification. Several algorithms have recently been developed in the mathematical research community, but their applicability and their interdependency has been studied in detail. This work is briefly summarized in Section II.
2) Integratation of the UQ algorithms in a user-friendly setup into TICRA Tools, such that UQ can be used across all existing TICRA products (GRASP, CHAMP 3D, ESTEAM, QUPES, POS).
3) Test the software across a range of cases. This is discussed in Section III.

II. Overview of Mathematical Techniques

We seek to quantify the behaviour of an antenna system as a function of the uncertainties in its design variables. The behaviour is expressed as an output with uncertainty (OwU), while the design variables are described as a set of stochastic uncorrelated variables.

Mathematically, we assume that the OwU is a deterministic function $F(\overline{X})$, where $\overline{X}$ is a set of N stochastic variables, assumed uncorrelated, with marginal distributions $g_{X^{(i)}}$, where $a^{(i)}$ and $b^{(i)}$ are the limits of this distribution function. We stress that a key aspect of this activity is that F is a black-box function, allowing us to apply the techniques described here in a non-intrusive manner, that is, without modifying the computation of F. Indeed F can represent any relevant output from the antenna system, which is a key strength of the techniques, as it allows users to inspect any quantity they

deem important for their specific application. Mathematically, we only assume the function to be a continuous function $F : \mathbb{R}^N \to \mathbb{R}$ that represents some OwU.

The most common distributions of the variables are shown in Table I. We will limit the possible variable distributions

TABLE I
THE MARGINAL DISTRIBUTIONS AVAILABLE IN THE SOFTWARE. NOTE THAT, $B(\alpha, \beta) = \Gamma(\alpha)\Gamma(\beta)/\Gamma(\alpha+\beta)$ IS A NORMALISATION CONSTANT.

Name	$\mathbf{g}_{\mathbf{X}^{(i)}}$	Support	Parameters
Uniform	$\frac{1}{b-a}$	$[a, b]$	$a < b$
Normal	$\frac{1}{\sigma\sqrt{2\pi}} e^{-\frac{1}{2}\left(\frac{x-\mu}{\sigma}\right)^2}$	$[-\infty, \infty]$	μ, $\sigma > 0$
Beta	$\frac{(x-a)^{\alpha-1}(b-x)^{\beta-1}}{(b-a)^{\alpha+\beta-1}B(\alpha,\beta)}$	$[a, b]$	$a < b$, $\alpha, \beta > 0$

to Normal, Uniform and Beta. However, in principle, any distribution can be treated, even discrete distributions. For simplicity, we will only consider continuous variables in the following.

We note that in practice, F is likely multi-variate, considering of M OwUs the system simultaneously. Since the computationally most demanding part of evaluating $F(\overline{X})$ is the analysis of the antenna itself, we stress that the antenna analysis is only done once, and then all M OwUs are extracted based on the results of the antenna analysis and treated as the result of independent stochastic processes. The object of the algorithms described here is to characterize these stochastic processes.

To allow the implementation of the accurate statistical estimates relevant for the present activity, we need to characterize the full conditional distribution of F, conditional on the variables $\overline{X}$. The distribution of F can be expressed in a number of different ways, e.g. by computation of its moments:

$$\textbf{Expected value}: \quad \mathrm{E}(F(\overline{X})) = \mu_F \tag{1}$$
$$= \int_{a^{(1)}}^{b^{(1)}} \int_{a^{(2)}}^{b^{(2)}} \cdots \int_{a^{(D)}}^{b^{(D)}} g_X(\overline{X}) F(\overline{X}) d\overline{X},$$
$$\textbf{Variance}: \quad \mathrm{Var}(F(\overline{X})) = \sigma_F^2 \tag{2}$$
$$= \int_{a^{(1)}}^{b^{(1)}} \int_{a^{(2)}}^{b^{(2)}} \cdots \int_{a^{(D)}}^{b^{(D)}} g_X(\overline{X}) F^2(\overline{X}) d\overline{X} - \mu_F^2,$$

or by approximating F by a function expansion

$$F(\overline{X}) \approx \sum_{i=1}^{K} \alpha_i f_i(\overline{X}), \tag{3}$$

and applying statistical analysis to that function expansion.

A. Methods for Uncertainty Quantification

There are several methods available for UQ, and the methods can roughly be classified as follows:

- Monte-Carlo based approaches,
- Intrusive Higher-Order methods,
- Non-intrusive Higher-Order methods

Since we consider F as a black-box function, Intrusive Higher-Order methods are not suitable [1, Section 10.2]. Hence, we have focused on a Monte-Carlo (MC) method in addition to two Non-intrusive Higher-Order methods, namely, Stochastic Collocation (SC) and Polynomial Chaos Expansion (PCE). Here, non-intrusive means that F is treated as a black-box function with the only requirement being that we should be able to evaluate it.

The methods are presented below in the following order:

1) Monte-Carlo
2) Stochastic Collocation
3) Polynomial Chaos Expansion

This order roughly reflects the complexity of implementation and the computation time required with Monte-Carlo being the simplest method. The three methods provide us with different information about F. The MC method provides function values at a number of samples of the input variables; these can be used to estimate the expected behaviour of the OwU and the expected deviation from this behaviour in addition to estimates of statistics like the confidence interval. The SC method provides an estimate of a number of moments of F, which again can be used to estimate the expected performance and its expected deviation; statistics like confidence intervals can be computed after an assumption is made about the distribution of F. The PCE method provides an approximation to F of the form (3), which can be used to get the relevant statistics (expected performance, deviation, confidence intervals) by sampling the approximation like with MC; in addition, the PCE method provides so-called Sobol indices [2, Section 4], which indicate the user the amount of variation in the OwU caused by the different variables. The methods are summarized below, and we refer to the Final Report for more in-depth details, including key implementation aspects.

1) Monte-Carlo: Monte-Carlo (MC) is an extremely simple method: Perform N_q evaluations of F, gather all the results in a vector $\overline{f}$, and compute the mean $\mu_F = \frac{1}{N_q}\sum_{i=1}^{N_q} f_i$ and the variance $\sigma_F^2 = \frac{1}{N_q - 1}\sum_{i=1}^{N_q}(f_i - \mu_F)^2$, although it should in practice be computed by a stable formula for variance computation, see e.g. [3] and the references therein.

From an accuracy and efficiency perspective, the difference in practice between the convergence rate of Monte-Carlo (MC) and higher-order methods is extreme for a moderate number of unknowns. One of the reasons that the convergence rate of MC is poor is that the method relies on completely random sampling which has high discrepancy, i.e., the samples have a tendency to cluster, rather than fill the function space. To mitigate the poor convergence, we use a sequence of low-discrepancy numbers instead of pseudo random numbers, such that the rate of convergence is increased from $\frac{1}{\sqrt{N_q}}$ to $\frac{1}{N_q}$. This approach is termed *Quasi-Monte-Carlo* (QMC) [4] and the low-discrepancy numbers are termed Quasi-random in the sense that they are deterministic (but long) sequences of numbers.

Still, even with the improvement of QMC over MC, the convergence of QMC is still much too slow compared to higher-order methods. From this it is clear that QMC should mainly be considered in cases where an independent verification is

necessary or when the number of variables makes the use of the higher-order methods too time-consuming.

2) Stochastic Collocation: The SC method approximates the moments of the function F by direct numerical integration, using specialized integration rules based on orthogonal polynomials as done in the Wiener-Askey scheme, but without actually producing a functional representation of F. In other words, F is only characterized by its moments. A brief overview is found in [1, Section 11.1] and [5, Chapter 7].

SC computes the moments directly, by numerically computing the integrals of F. As an illustration of the method, we consider the computation of the first moment (1). Clearly, this is an N-dimensional integral against a kernel, namely the probability density of the variables g_X. From approximation theory, see e.g. [5, Chapter 3], we understand that the optimal integration rule for such an integral is found by applying Gaussian quadrature rules constructed to be orthogonal relative to the measure induced by g_X. Hence, the moments can be computed by numerical quadrature as follows:

$$\mu_F \approx \sum_{q=1}^{N_q} F(\overline{X}_q) w_q, \tag{4}$$

$$\sigma_F^2 \approx \sum_{q=1}^{N_q} F(\overline{X}_q)^2 w_q - \mu_F, \tag{5}$$

and so on for the higher moments if relevant.

We can then use the computed moments "as is", as key statistics of our function. To compute more sophisticated statistics, such as confidence intervals, we construct a cumulative distribution function for F conditioned on the distribution of $\overline{X}$, based on the available moments.

The advantages of SC when used for UQ is clearly the simplicity of implementation, which relegates the majority of the complexity to the task of accurately performing N-dimensional numerical quadrature. The main drawback, relative to the next method, is the restriction to a preselected distribution family.

To get the moments of F, we perform successively more accurate integration based on different quadrature rules and judge convergence along the way. The choice of (N-dimensional) quadrature scheme is no easy task and good quadrature rules depend on the distributions of the variables. For example, when all variables are uniformly distributed a set of efficient integration rules known as the Stroud rules [6] are at our disposal but only up to a certain accuracy. A more general quadrature scheme is the sparse grid rules [1], [7, Section 11], where the accuracy can be increased and the number of points required in more dimensions does not grow too fast.

3) Polynomial Chaos Expansion: Polynomial Chaos Expansion (PCE) is a method that approximates the behaviour of the function F by an expansion of orthogonal polynomials in each variable. More details about the method can be found in [2], [8]–[11].

The key concept for a PCE is the approximation of F as a sum of orthogonal polynomials, the so-called polynomial chaos basis. The construction of these polynomials is trivial in the univariate case $N = 1$, but in the multi-variate case, it becomes non-trivial as the maximum order of the multi-variate terms can be controlled independently from the order of the univariate terms.

The P'th order polynomial chaos expansion of a function F evaluated at a specific point $\overline{X}$ can be expressed as

$$F(\overline{X}) \approx \sum_{t=0}^{K} \alpha_t \Psi_t(\overline{X}), \tag{6}$$

Where $K = \frac{(N+P)!}{N!P!} - 1$ and the polynomial chaos basis functions are expressed as Ψ_t. This scheme is termed the Wiener-Askey scheme and is discussed in more detail in [12].

With the expansion (6) we are thus, in contrast to the Stochastic Collocation method, directly able to calculate the value of our approximation to F at any $\overline{X}$ by simply evaluating (6). What remains is the computation of the coefficients α_t, which is in principle done by projection of the full expansion against F, although more sophisticated methods provide better results.

This description allows us to compute every statistic that we can compute with SC. Further, PCE allows us to extract more information than SC. First, since we have a full description of F, we can avoid the need for a predetermined distribution and simply compute directly the PDF or CDF of F by Monte-Carlo analysis of (6), which is very fast since it requires evaluation only of simple polynomials.

Secondly, the PCE allows the extraction of individual parameter uncertainties by computation of the so-called Sobol indices, as discussed in [2]. The most intuitive of these are the first-order Sobol indices, which constitute the conditional variances conditioned on the variation of a single variable, but in principle higher-order conditional variances (conditioned on variation of multiple variables simultaneously) can be extracted as well. This can be a very important piece of information in practice. The first-order Sobol index for the ith variable is computed as

$$S_i = \frac{\sum_{t \in T_i} \alpha_t^2 Q_t}{\sigma^2}, \tag{7}$$

where T_i is the set of indices where the chaos polynomial only contains powers of variable i.

Thus, with PCE, the user can not only learn an accurate estimation of the statistical behaviour of F over all variables $\overline{X}$ — typically more accurately than for SC due to the lack of requirement for a predetermined distribution — but can also learn the main reasons of this variation by inspecting the Sobol indices that indicate which variable (or set of variables) are responsible for how much of the variation. This, for instance, allows for cost-based uncertainty reduction of a system. For instance, if it turns out that a single variable is responsible for, say, 80% of the variation in the performance, it is clear that it will be worthwhile increasing the reliability of that variable.

III. Application Examples

As part of the activity 6 test cases were defined, see [13], with which to validate the developed software. The application of the software to these cases were the topic of [14]. Three of these test cases have been selected as examples for this document and are presented in the following.

A. Example 1: Multi-Beam Reflector Antenna System

This topic of this example is an antenna system that may find application for a so-called High-Throughput-Satellite (HTS). Specifically it is a 4-colour multi-beam single-feed-per-beam configuration. The beams of the antenna system are shown in Figure 1. Each antenna has a single offset reflector with a diameter of $3.66\,\mathrm{m}$ and operates at a frequency of 30 GHz. The beam width is $0.25°$. In such systems, it is important that the sidelobes of one beam in the nearest neighbouring coverage cell with the same frequency and polarisation are not too high, to avoid compromising the C/I (Carrier to Interference) ratio. For the present, we focus on a single reflector generating a single color.

This means that the most interesting cell to look at begins $0.375°$ away from the peak. In Figure 2 the beam of this configuration, centred at $\theta = 0°$, is shown with the beam on the opposite side of the nearest neighbour. The nearest neighbour is "off-colour" (a different frequency or polarisation) meaning there will not be noteworthy interference with this. However, the "next-neighbour" beam has the same colour and there will be mutual interference between this and the centre beam. With respect to the coordinate systems used in Figure 2 this means that the radiation patterns of the central beam should not unduly interfere in the directions defined by $\theta \in [0.375°; 0.625°]$. To this end the radiation in this range will be subject to analysis wrt. the influence of surface deformation of the reflector's shape and mounting angles.

In [14], additional investigations involving variations of the reflector shape and coupling between the feed of the two beam were presented. These are omitted here and presently variations of the reflector's orientation is addressed. With only the 3 orientation variables a Monte Carlo analysis of this problem is feasible and thus reference data has been generated using 20.000 samples. The orientations are varied according to a normal distribution with a standard deviation of $\sigma = 0.01°$. The aim is now to recover the expected mean and 95% confidence interval for this case using the Polynomial Chaos Expansion method.

In Figure 3 the 95% confidence interval and the expected mean of the radiation pattern are shown and compared with the Monte Carlo reference. The Polynomial Chaos Expansion was employed using a dynamic range of 30 dB within a θ-range from $0.3°$ to $0.7°$, which means that it aims at ensuring convergence at levels less than 30 dB below the value at $0.3°$, i.e., in the present case about a level of 5 dBi.

Inspection of the plots shows that the obtained results agree fairly well with the reference results. The curves deviate slightly for the lower bound of the confidence interval with a maximum deviation of about 0.4 dB at a level around 12 dBi (18 dB below peak). This result was obtained after 1097 function evaluations (samples) in the Polynomial Chaos Expansion method.

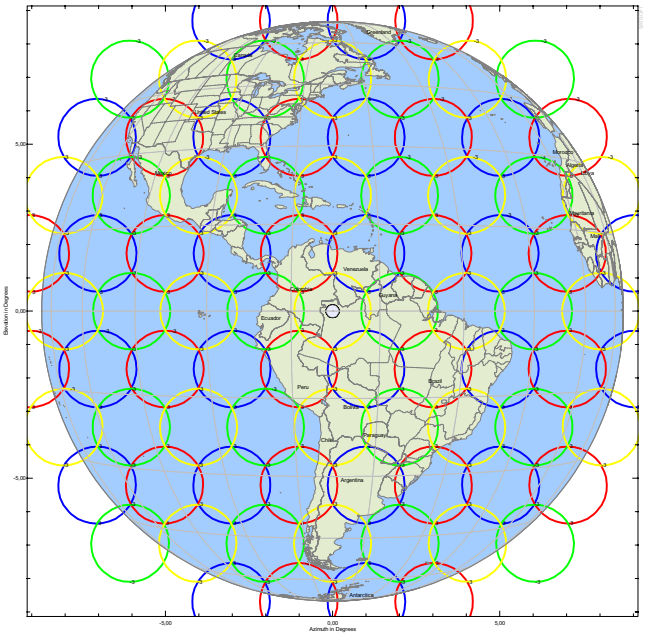

Fig. 1. The beams from the HTS used in Example 1. Beams with the same colour have the same polarisation and frequency and are generated by offset feeds using the same reflector.

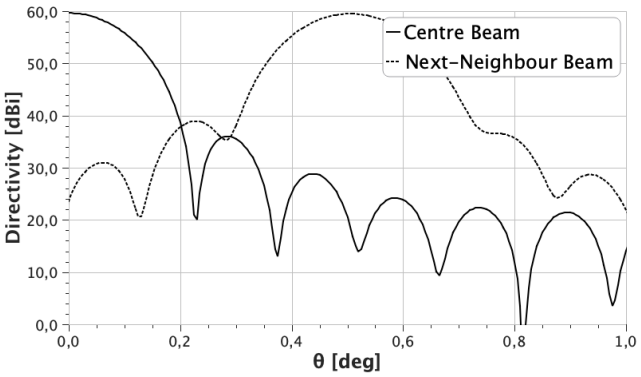

Fig. 2. Nominal radiation patterns of two beams. The centre beam is shown with the "next-neighbour" beam at $\theta = 0.5°$ (same colour).

B. Example 2: Reflectarray Mounted on Cubesat

In many practical cases, the influence of a nearby satellite body can affect antenna performance negatively. We therefore include an example where the platform has a very large impact on the antenna performance - the deployable reflectarray shown in Figure 4 is such a case. The flush-mounted all-metallic feed employs the entire top face as an inherent part of the feeding structure. The reflectarray consists of three deployable panels with spring-loaded hinges and each panel is constructed as a symmetric set of Rogers substrates around a glass fibre core. In total the 1703 cross-shaped reflectarray ele-

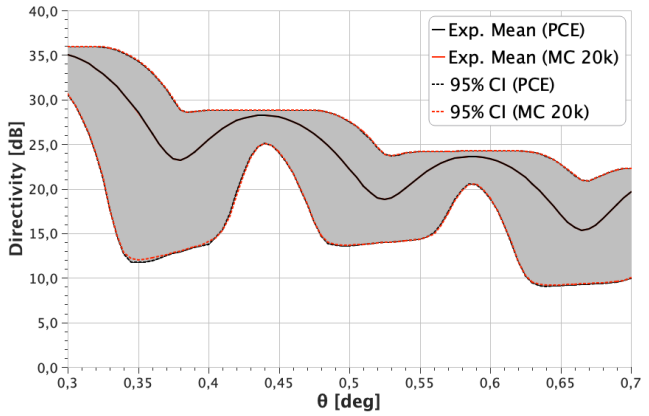

Fig. 3. Radiation patterns predicted by Polynomial Chaos Expansion compared with Monte Carlo using 20.000 samples. The Confidence interval is shown in grey.

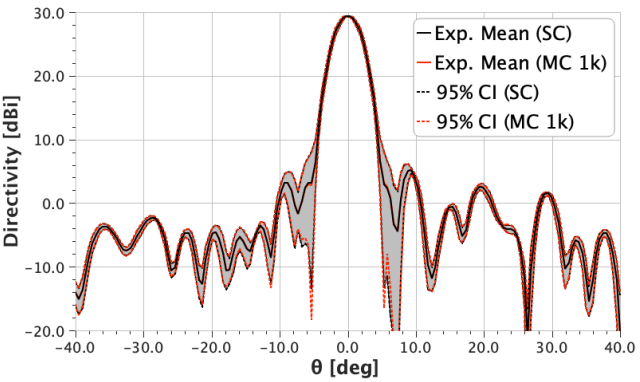

Fig. 5. Radiation pattern with associated confidence interval predicted by Stochastic Collocation compared with Monte Carlo using 1.000 samples. The Confidence interval is shown in grey.

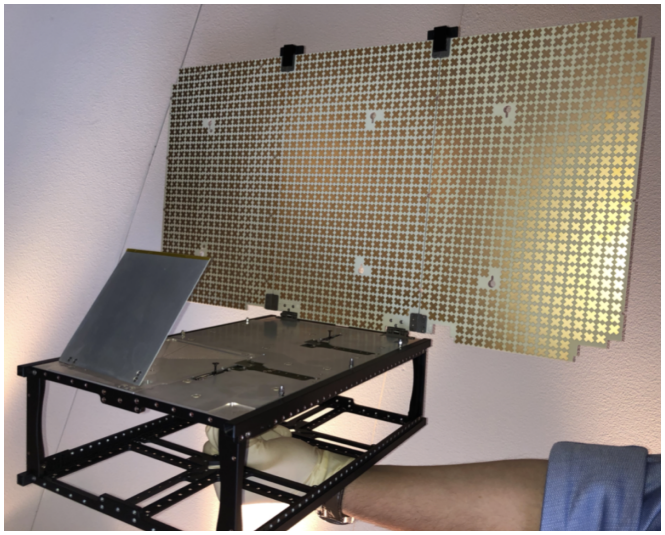

Fig. 4. Deployable reflectarray on a 6U cubesat.

ments are positioned on the 3 panels. The reflectarray operates at X-band from 8.0 - 8.4 GHz. Depending on the analysis to be done different computational models are relevant. In the right-hand side of Figure 4 an example of such a model is shown. In that model the feed, which is embedded in the top face of the satellite can be seen with the 3 panels of the reflectarray.

Variable	Amount	Distribution	Tolerance
ψ_L, ψ_R	2	Uniform	$\pm 0.2°$
ψ_C	1	Uniform	$\pm 0.4°$
ψ_F	1	Uniform	$\pm 0.5°$
ϵ_s	1	Normal	± 0.05 ($\pm 1\sigma$)
t_s	1	Normal	± 0.01 mm ($\pm 1\sigma$)
δ_i	5109	Uniform	± 0.02 mm

TABLE II
SUMMARY OF VARIABLES AND THEIR DISTRIBUTIONS USED IN EXAMPLE 2.

This investigation relates to the hinge deployment angles of the reflectarray panels and the feed plate. Obviously an accurate deployment of the panels is a prerequisite for succesful communication with the satellite. Severe errors and possibly malfunction of the antenna may result if the hinges fails to open flawlessly. The deployment angles ψ_L, ψ_R, ψ_C, and ψ_F of the left, right, centre, and feed hinges, respectively, are therefore relevant quantities to investigate in an uncertainty quantification analysis. The angles are varied according to Table II and the Stochastic Collocation method is employed in the analysis. A reference solution has been obtained using the Monte Carlo method with 1000 samples. With only 4 variables this is assumed to have converged.

The result obtained by Stochastic Collocation is shown in Figure 5 where it is compared with the Monte Carlo reference. The co-polar directivity of the reflectarray antenna is shown for $\phi = 90°$. Note that the Stochastic Collocation analysis is done with convergence requirements down to 30 dB below the peak value on the co-polar component. Hence it may be expected, that the method recovers the Monte Carlo reference data down to a level of about 0 dBi. The maximum deviation for the expected mean are less than 0.01 dBi around the peak and 0.3 dBi in the off-peak parts. Corresponding values for the confidence interval are about 0.01 dBi around the peak and 0.4 dBi in the off-peak parts.

This second investigation relates to manufacturing errors of the substrate thickness t_s and permittivity ϵ_s as well as the etching of the 1703 cross-shaped elements, denoted by δ_i. This totals 5111 variables as listed in Table II. A converged Monte Carlo reference result is not feasible for this analysis because there are simply too many variables. Instead so-called Ensemble reference data is generated using 10.000 samples. This means that 10.000 random samples are generated and the resulting output is used as reference when assessing the correctness of the method. The obtained Ensemble values of the co- and cross-polar directivities at $\theta = 0°$ are shown in Figure 6 as black dots. Super-imposed on these are the associated 95% confidence intervals predicted by the Stochastic Collocation. It is then the aim that roughly 95% of the black dots should be encompassed by the predicted confidence

intervals. A detailed count of the black dots reveal that the confidence intervals encompass about 98% and 92% of the samples, for the co- and cross-polar directivities, respectively. The above results were obtained using roughly 15.300 function evaluations, i.e., samples of the etching errors δ_i and substrate errors ϵ_s and t_s.

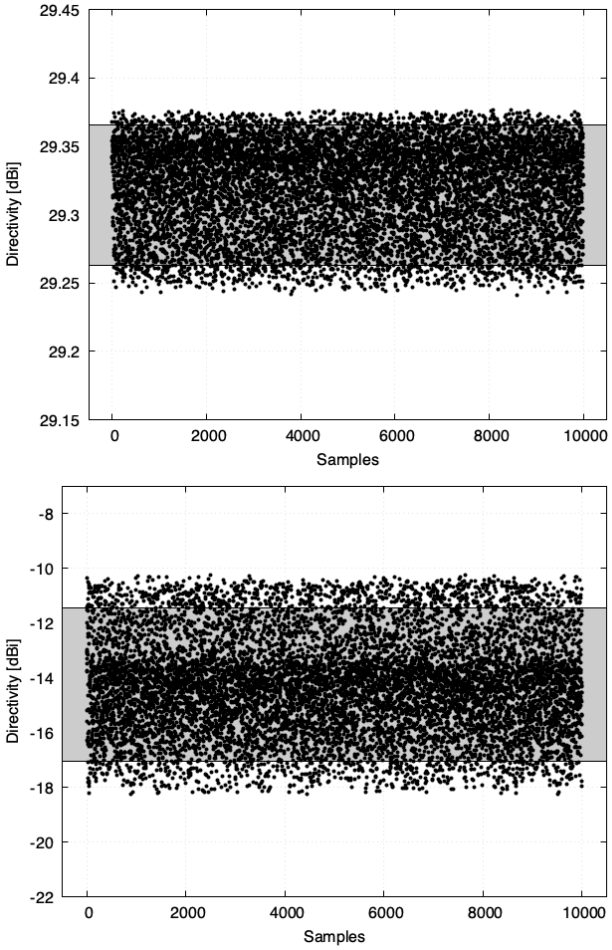

Fig. 6. Co- and cross-polar directivities at $\theta = 0°$ sampled 10.000 times with varying values of the substrate and element etching as listed in Table II. Confidence intervals are shown in grey.

C. Example 3: Corrugated Horn Antenna

In this example a corrugated horn antenna is analysed. This kind of antenna is commonly used as a reflector feed. The horn includes 18 slanted radial corrugations as indicated in Figure 7. The operating frequency of the horn is 10 GHz.

The horn profile may present challenges in terms of manufacture. Particularly a specified accuracy of the slanted corrugations may be difficult to maintain depending on wear and accuracy of the employed machinery. It is therefore relevant to have an idea of the impact of such inaccuracies. The 18 corrugations are varied with respect to widths and depths giving rise to 36 variables, 18 depth errors d_i and 18 width errors w_i. In addition the flare angle α and two alignment

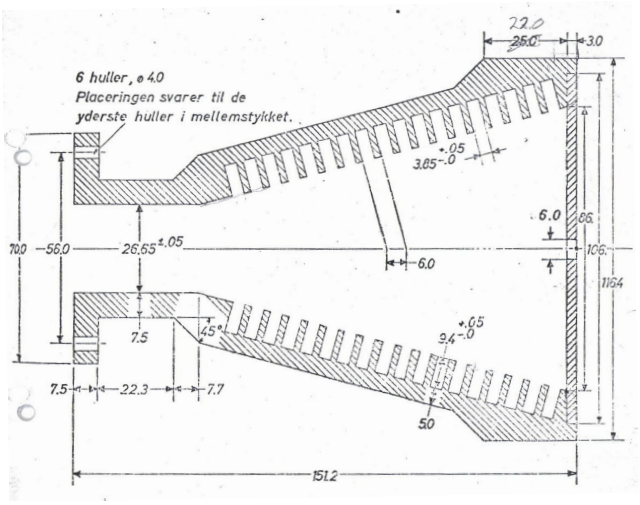

Fig. 7. Profile of the corrugated horn antenna with slanted corrugations.

angles β and ϕ are varied. In Table III the variables and their distributions are summarised.

Variable	Amount	Distribution	Tolerance
d_i	18	Uniform	± 0.1 mm
w_i	18	Uniform	± 0.1 mm
α	1	Uniform	$\pm 0.5°$
β	1	Normal	$\pm 0.5°$ ($\pm 1\sigma$)
ψ	1	Normal	$\pm 0.5°$ ($\pm 1\sigma$)

TABLE III
SUMMARY OF VARIABLES AND THEIR DISTRIBUTIONS USED IN EXAMPLE 3.

The first investigation is done using the Polynomial Chaos Expansion in an analysis of the radiation pattern of the antenna when this is oriented with small alignment errors β and ψ as summarised in Table III. For comparison a corresponding analysis has been done using the Monte Carlo method with 10.000 samples of the two alignment angles β, ψ. With only two variables, it is assumed that the Monte Carlo method has converged. In Figure 8 the directivity of the antenna is shown for $\phi = 45°$. Note that the Polynomial Chaos Expansion analysis is done with convergence requirements down to 40 dB below the peak value. Hence it may be expected, that the method recovers the Monte Carlo reference data down to a level of about -22 dBi. It is seen that the results are in very good agreement with very small errors. Since the Polynomial Chaos Expansion is not expected to provide correct results for levels below -22 dBi, some deviations for values lower than this are acceptable as is for example seen in the plot of the cross-polar component. We note that these results were obtained with just 41 function evaluations, i.e., samples of the alignment angles.

The second investigation relates the peak directivity and reflection coefficient. This is analysed including all 37 variables related to the manufacturing tolerances in Table III, i.e., excluding the alignment angles. The reference data consist of an Ensemble of 1000 random samples and in Figure 9 the

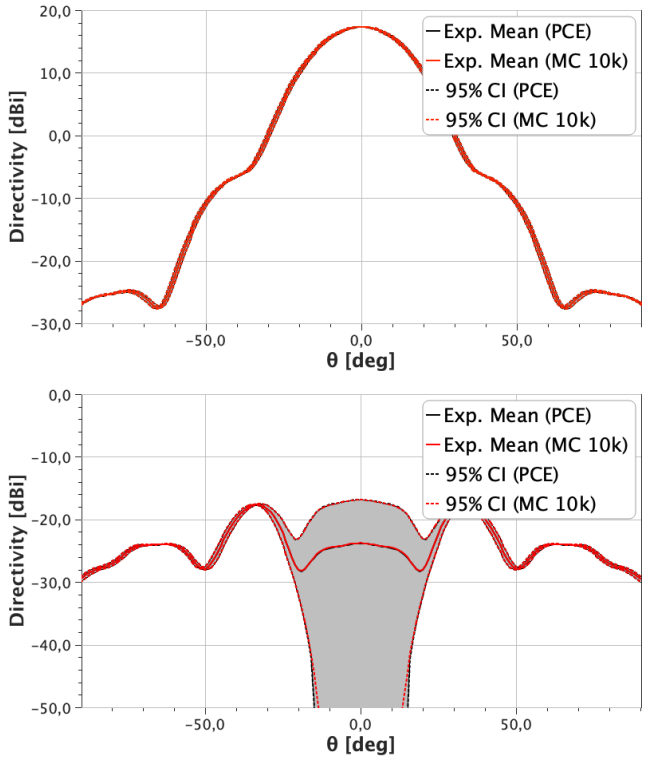

Fig. 8. Co-polar (top) and cross-polar (bottom) radiation patterns at $\phi = 45°$ of the corrugated horn with alignment errors of β, ψ at 10 GHz predicted by Polynomial Chaos Expansion compared with Monte Carlo using 10.000 samples. Confidence intervals are shown in grey.

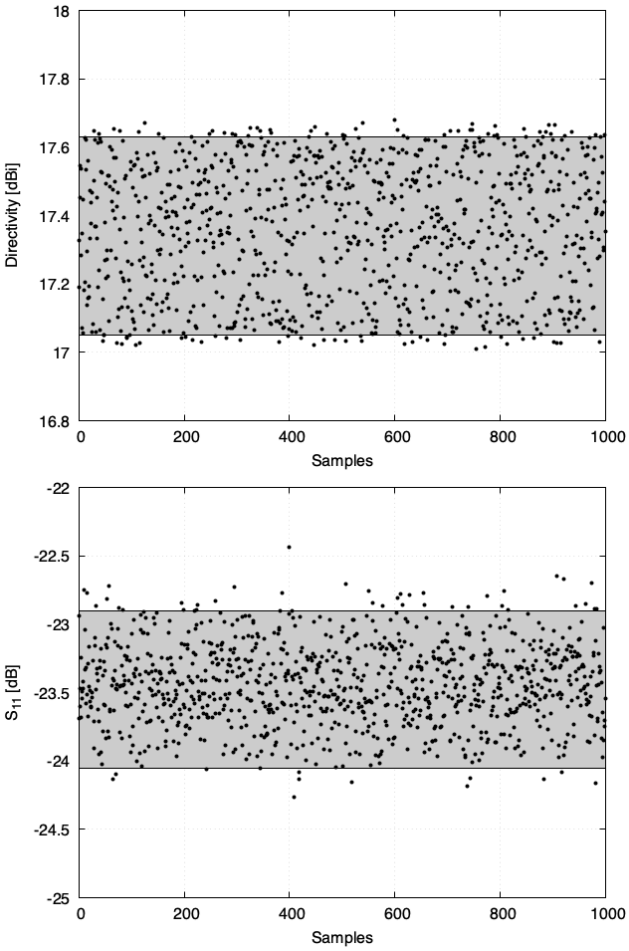

Fig. 9. Peak directivity and reflection coefficient sampled 1000 times with varying values of the mechanical errors as listed in Table III. Confidence intervals are shown in grey.

corresponding values of the peak directivity and reflection coefficient at 10 GHz are shown. Again, the 95% confidence interval, predicted by Stochastic Collocation, is super imposed. It is noted that the confidence intervals encompass 91% and 95% of the samples, for the co- and cross-polar directivities, respectively. These results were obtained with just 112 function evaluations, i.e., samples of α, β, and ψ.

IV. Conclusions and Perspectives

The perspectives at the outset of this activity were quite daunting: build a completely novel addition to the TICRA Tools software family that allows, for any design that can be analysed using the TICRA Tools algorithms, the user to easily, rapidly and reliably compute statistics such as confidence intervals for the effect of production uncertainties.

None-the-less, this challenge has been met. The output of this activity is first and foremost software that allows the user to do just that. The software is

1) Easy-to-use: For users familiar with the TICRA Tools framework, all that is needed is to specify the distribution of the variables and the output of interest. Most everything else is handled automatically, while the user can (but is not forced to) easily control a few additional parameters.
2) Fast: With advanced UQ algorithms focused on minimizing the computational resources spent, the user is able to analyse several different designs in fractions of the time needed for the industry-standard Monte-Carlo alternatives to the software.
3) Reliable: The UQ algorithms provide accurate and reliable statistical output, meaning that users can trust that the information such as confidence intervals are realistic.

With these properties, we are confident that a wide range of antenna engineers including designers, manufacturers and operators will find the software applicable in their daily work.

This assessment is also confirmed by the fact that TICRA has already put in a vast amount of development resources beyond this contract to further strengthen the UQ software. We are currently aiming to release the software to our users within 6 months of the completion of this contract.

References

[1] R. C. Smith, *Uncertainty Quantification: Theory, Implementation, and Applications*. USA: Society for Industrial and Applied Mathematics, 2013.

[2] T. Crestaux, O. L. Maıˆtre, and J.-M. Martinez, "Polynomial chaos expansion for sensitivity analysis," *Reliability Engineering & System Safety*, vol. 94, no. 7, pp. 1161 – 1172, 2009,

special Issue on Sensitivity Analysis. [Online]. Available: http://www.sciencedirect.com/science/article/pii/S0951832008002561

[3] E. Schubert and M. Gertz, "Numerically stable parallel computation of (co-) variance," in *Proceedings of the 30th International Conference on Scientific and Statistical Database Management*. ACM, 2018, p. 10.

[4] H. Niederreiter, "Quasi-monte carlo methods and pseudo-random numbers," *Bulletin of the American mathematical society*, vol. 84, no. 6, pp. 957–1041, 1978.

[5] D. Xiu, *Numerical Methods for Stochastic Computations: A Spectral Method Approach*. Princeton University Press, 2010. [Online]. Available: https://books.google.fr/books?id=GY9qyJd4CvQC

[6] A. H. Stroud, "Remarks on the disposition of points in numerical integration formulas," *Mathematical Tables and Other Aids to Computation*, 1957.

[7] T. Gerstner and M. Griebel, "Numerical integration using sparse grids," *Numerical algorithms*, vol. 18, no. 3, pp. 209–232, 1998.

[8] L. Ng and M. S. Eldred, "Multifidelity uncertainty quantification using nonintrusive polynomial chaos and stochastic collocation," in *AIAA/ASME/ASCE/AHS/ASC Structures, Structural Dynamics and Materials Conference*, 2012.

[9] A. C. M. Austin and C. D. Sarris, "Efficient Analysis of Geometrical Uncertainty in the FDTD Method Using Polynomial Chaos With Application to Microwave Circuits," *IEEE Transactions on Microwave Theory and Techniques*, vol. 61, no. 12, pp. 4293–4301, Dec. 2013.

[10] A. C. M. Austin, N. Sood, J. Siu, and C. D. Sarris, "Application of Polynomial Chaos to Quantify Uncertainty in Deterministic Channel Models," *IEEE Transactions on Antennas and Propagation*, vol. 61, no. 11, pp. 5754–5761, Nov. 2013.

[11] B. Sudret, S. Marelli, and J. Wiart, "Surrogate models for uncertainty quantification: An overview," in *2017 11th European Conference on Antennas and Propagation (EUCAP)*. Paris, France: IEEE, Mar. 2017, pp. 793–797.

[12] D. Xiu and G. E. Karniadakis, "The wiener–askey polynomial chaos for stochastic differential equations," *SIAM Journal on Scientific Computing*, vol. 24, no. 2, pp. 619–644, 2002.

[13] Advanced Antenna Modelling Tool for Performance Verification and Diagnosis - TN2, *S-1691-TN2*, TICRA, Copenhagen, Denmark, 2021.

[14] Advanced Antenna Modelling Tool for Performance Verification and Diagnosis - TN3, *S-1691-TN3*, TICRA, Copenhagen, Denmark, 2021.